ACS Catalysis

RESEARCH ARTICLE

pubs.acs.org/acscatalysis

Hydrogenation of Carbon Dioxide Catalyzed by PNP Pincer Iridium, Iron, and Cobalt Complexes: A Computational Design of Base Metal Catalysts

Xinzheng Yang*

Molecular Graphics and Computation Facility, College of Chemistry, University of California, Berkeley, California 94720, United States

Supporting Information

ABSTRACT: The reaction mechanisms for hydrogenation of carbon dioxide catalyzed by PNP-ligated (PNP = 2,6-bis(di-*iso*-propylphosphinomethyl)pyridine) metal pincer complexes, (PNP)IrH_3 (**1-Ir**), *trans*-(PNP)$Fe(H)_2CO$ (**1-Fe**) and (PNP)-CoH_3 (**1-Co**), were studied computationally by using the density functional theory (DFT). **1-Ir** is a recently reported high efficiency catalyst for the formation of formic acid from H_2 and CO_2. **1-Fe** and **1-Co** are computationally designed low-cost base metal complexes for catalytic CO_2 reduction. For the formation of formic acid from H_2 and CO_2 catalyzed by **1-Ir**, **1-Fe**, and **1-Co**, the reaction pathways with direct H_2 cleavage by OH^- without the participation of the PNP ligand are about 20 kcal mol^{-1} more favorable than a previously postulated H_2 cleavage mechanism that involves the aromatization and dearomatization of the pyridine ring in the PNP ligand. This finding reveals the essential role of the base, OH^-, in the catalytic CO_2 reduction cycle and suggests that the incorporation of strong bases and unsaturated ligands may be critical for new catalyst design in the area of hydrogen activation and low energy proton transfers. The calculated overall enthalpy barriers for the formation of formic acid from H_2 and CO_2 catalyzed by **1-Ir**, **1-Fe**, and **1-Co** are 18.6, 21.9, and 22.6 kcal mol^{-1}, respectively. Such low barriers explain the observed unprecedented high catalytic acitivity of **1-Ir** and indicate that **1-Fe** and **1-Co** can be considered as promising low-cost catalyst candidates for fast hydrogenation of CO_2.

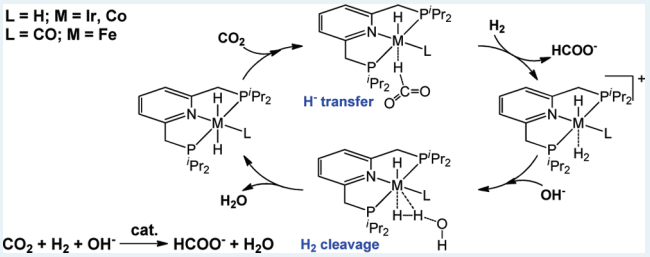

KEYWORDS: carbon dioxide, hydrogenation, homogeneous catalysis, catalytic mechanism, iridium, iron, cobalt, molecular modeling, catalyst design, density functional theory

INTRODUCTION

With the growing concentration of carbon dioxide in the Earth's atmosphere and the potential link to global climate phenomena, the reutilization of carbon dioxide as an abundant, inexpensive, and nontoxic carbon source for the synthesis of valuable chemicals has attracted increasing attention in recent decades.[1,2] Formic acid, for instance, is one possible target molecule because of its significant importance in synthetic chemistry and its potential applications in hydrogen storage. To overcome the low activity of carbon dioxide, transition metal catalyzed hydrogenation of CO_2 to formic acid and its derivatives has been studied extensively.[3−9] In most of these catalytic reactions, the presence of base is critical to make the hydrogenation of CO_2 to formic acid thermodynamically favorable. Very recently, Nozaki and co-workers reported a PNP-ligated (PNP = 2,6-bis(di-*iso*-propylphosphinomethyl)pyridine) iridium(III) trihyride complex, (^{i}PrPNP)IrH_3 (**1-Ir**), which achieves unprecedented catalytic activity with the turnover frequency (TOF) and turnover number (TON) values of 150 000 h^{-1} and 3 500 000 for the formation of HCOOK from CO_2 and H_2 in aqueous KOH.[10] Later on, Ahlquist computationally studied the mechanism of this catalytic CO_2 hydrogenation reaction using density functional theory (DFT) for a very simplified model structure, (PNP)IrH_3, in which iso-propyl groups were replaced by hydrogens to reduce the computational cost.[11] However, such a simplification does not take into account the steric and electronic effects of iso-propyl groups and led to a rather high overall free energy barrier of 26.1 kcal mol^{-1}.[11]

Although a very high efficiency has been achieved in catalytic hydrogenation of CO_2, the scarcity and cost of noble metals like iridium, ruthenium, and rhodium in reported catalysts are currently major factors preventing their large-scale practical application.[7] Several base metal catalysts for homogeneous CO_2 hydrogenation were reported in recent years.[12,13] However, these catalysts require high pressure H_2 and CO_2 (40−60 atm) for the reactions and have very low TOF. Therefore, the design of low-cost, high efficiency, and environmentally friendly base metal catalysts for hydrogenation reactions, while challenging, remains highly attractive.[14−17]

With extraordinary improvements in DFT in recent years, the computational design of new catalysts is making steady and promising progress.[18−22] In this paper, inspired by the structure

Received: January 20, 2011
Revised: March 15, 2011
Published: June 03, 2011

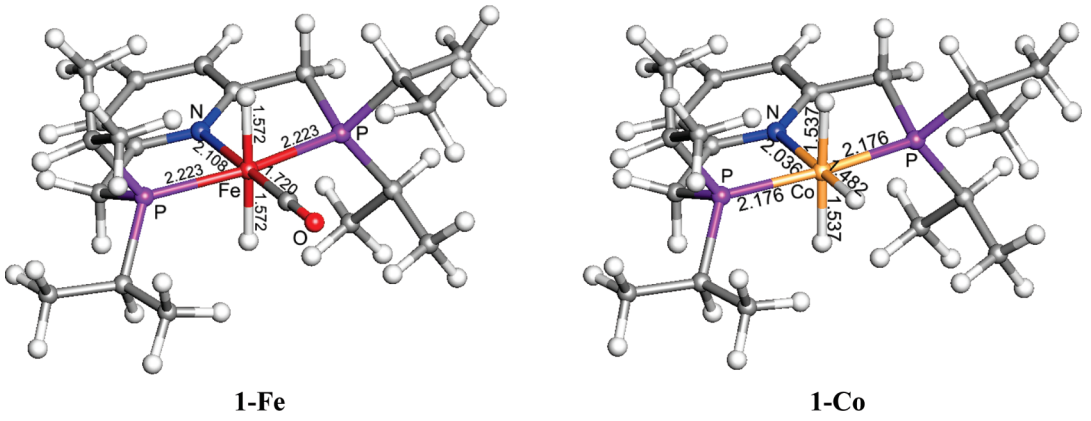

Figure 1. Optimized structure of newly designed PNP-ligated iron and cobalt complexes **1-Fe** and **1-Co**. Bond lengths are in angstroms.

Scheme 1. Predicted Reaction Mechanism for the Formation of Formic Acid from H_2 and CO_2 Catalyzed by 1-M (M = Ir, Fe, and Co) Showing OH^- Triggered H_2 Cleavage

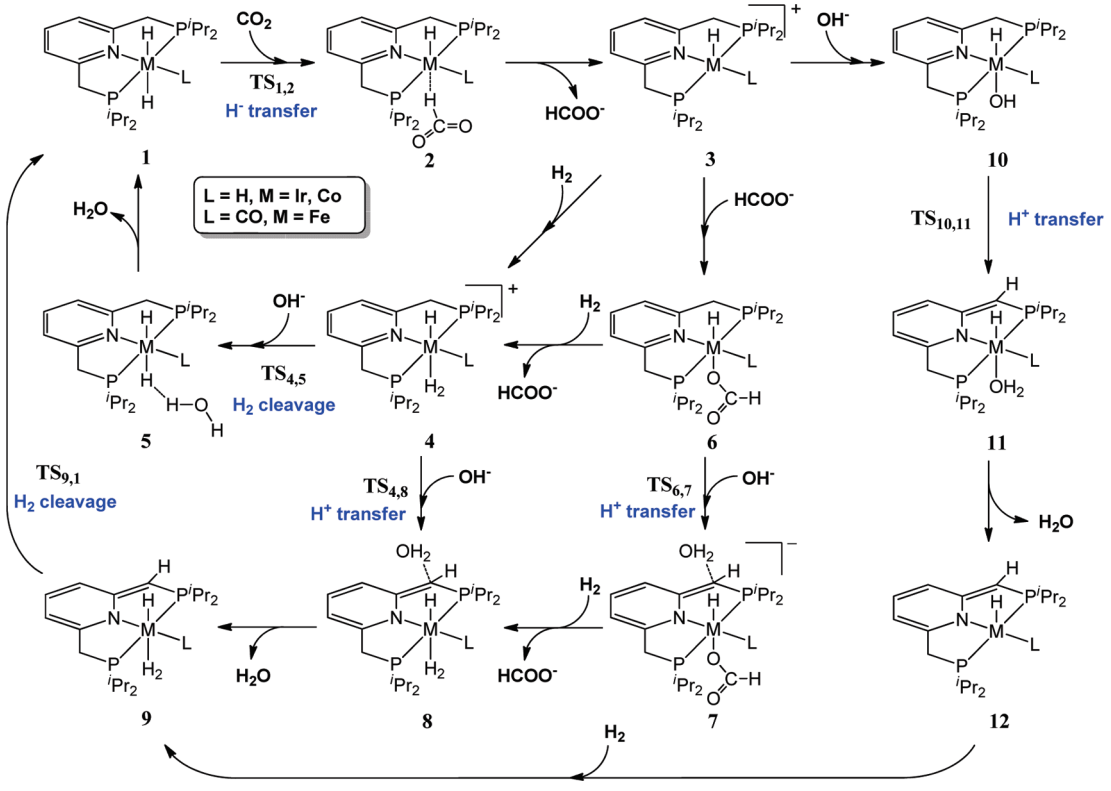

and understanding of the catalytic mechanism of (^{i}PrPNP)IrH_3, as well as the reported cobalt[23,24] and iron[25−28] complexes with similar pincer ligands, two new base metal complexes with the same ^{i}PrPNP pincer ligand, *trans*-(^{i}PrPNP)$Fe(H)_2CO$ (**1-Fe**) and (^{i}PrPNP)CoH_3 (**1-Co**) are examined computationally. The detailed mechanisms of **1-Ir**, **1-Fe**, and **1-Co** catalyzed $HCOO^-$ formation from H_2 and CO_2 in the presence of OH^- are studied by DFT. On the basis of detailed analysis of the catalytic mechanisms of these three complexes, **1-Fe** and **1-Co** are proposed as promising low-cost catalyst candidates for fast CO_2 reduction. It is worth noting that when this paper was being finalized, **1-Fe** was synthesized experimentally by Milstein and co-workers in their study of hydrogenation of ketones catalyzed by iron pincer complexes.[29]

COMPUTATIONAL DETAILS

All DFT calculations were performed using the Gaussian 09 suite of ab initio programs[30] at the long-range corrected hybrid functional ωB97X[31] and all-electron 6-31++G(d,p) basis set for all atoms[32−34](Stuttgart relativistic effective core potential basis set, ECP60MWB, for the Ir atom[35,36]) level of theory. An ultrafine integration grid (99,590) was used for numerical integrations. All structures studied in this paper were optimized

dx.doi.org/10.1021/cs2000329 |*ACS Catal.* 2011, 1, 849–854

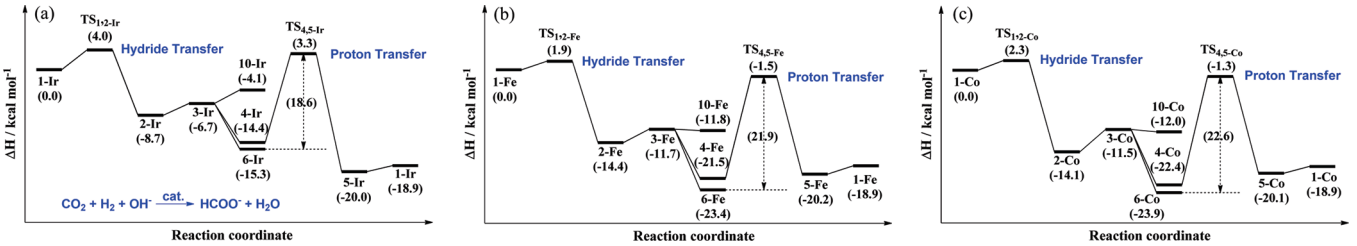

Figure 2. Solvent corrected enthalpy profiles of the catalytic cycles for the formation of formic acid from H_2 and CO_2 catalyzed by (a) **1-Ir**, (b) **1-Fe**, and (c) **1-Co** with direct H_2 cleavage by OH^- for H_2O formation without the participation of the PNP ligand.

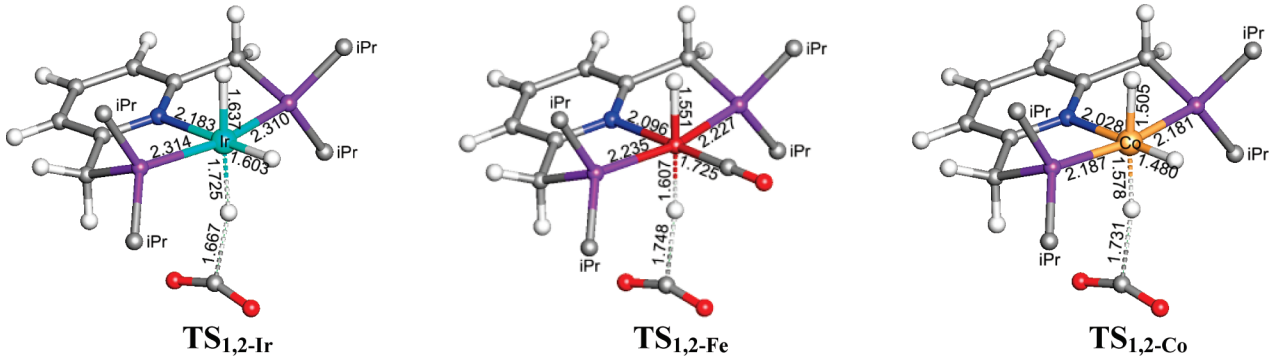

Figure 3. Optimized structures of $\mathbf{TS_{1,2\text{-}Ir}}$ (710*i* cm^{-1}), $\mathbf{TS_{1,2\text{-}Fe}}$ (616*i* cm^{-1}), and $\mathbf{TS_{1,2\text{-}Co}}$ (647*i* cm^{-1}). Bond lengths are in angstroms. Iso-propyl groups are not shown for clarity.

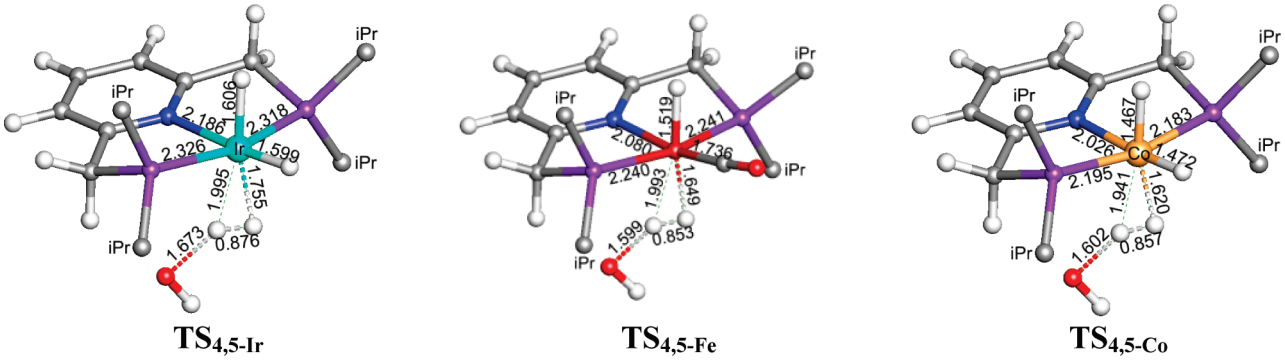

Figure 4. Optimized structures of $\mathbf{TS_{4,5\text{-}Ir}}$ (605*i* cm^{-1}), $\mathbf{TS_{4,5\text{-}Fe}}$ (693*i* cm^{-1}), and $\mathbf{TS_{4,5\text{-}Co}}$ (650*i* cm^{-1}). Bond lengths are in angstroms. Iso-propyl groups are not shown for clarity.

with solvent corrections using the integral equation formalism of the polarizable continuum model (IEFPCM)[37] with Bondi radii[38] for water. The ground states of intermediates were confirmed as singlets through comparison with the optimized high-spin analogues. Thermal corrections were calculated within the harmonic potential approximation on optimized structures under T = 298.15 K and 1 atm pressure. All calculated metal complexes have full-size ^{i}PrPNP ligands without simplification. Calculating the harmonic vibrational frequencies for optimized structures and noting the number of imaginary frequencies (IFs) confirmed the nature of all intermediates (no IF) and transition state structures (only one IF). The latter were also confirmed to connect reactants and products by intrinsic reaction coordinate calculations. The 3D molecular structure figures displayed in this paper were drawn by using the JIMP2 molecular visualizing and manipulating program.[39]

In view of the critical role of solvent in ion involved reactions, solvent corrected electronic energies were also calculated with the united atom topological model applied on radii (UAKS radii) for optimized structures. Then the solvent corrected enthalpies were obtained by adding the thermal enthalpy corrections to the solvent corrected electronic energies. The reliability of the solvent effect corrections using IEFPCM with both the UAKS and Bondi atomic radii is evaluated in the Supporting Information. Unless otherwise noted, the energies in the text are solvent corrected enthalpies.

RESULTS AND DISCUSSION

The optimized structures of the newly designed base metal complexes **1-Fe** and **1-Co** are shown in Figure 1. Although the calculated reaction energy barriers of **1-Ir**, **1-Fe**, and **1-Co**

dx.doi.org/10.1021/cs2000329 |ACS Catal. 2011, 1, 849–854

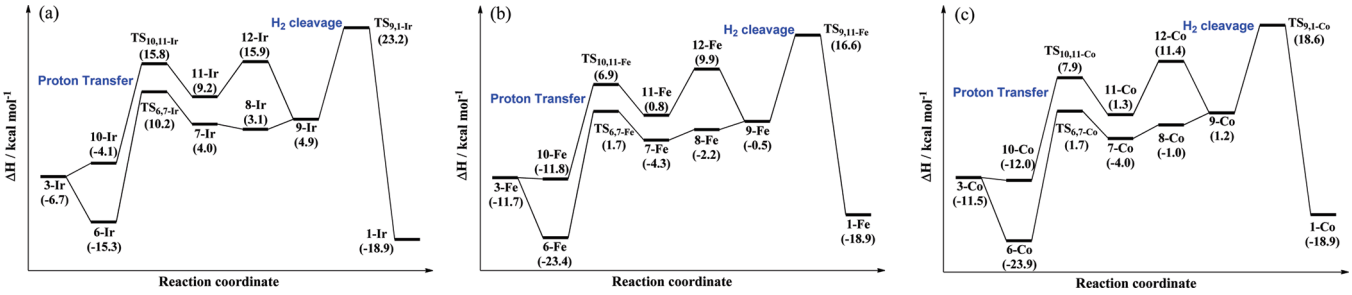

Figure 5. Enthalpy profiles for the reaction pathways with OH^- triggered the dearomatization and rearomatization of the pyridine ring in (a) **1-Ir**, (b) **1-Fe**, and (c) **1-Co** for H_2 cleavage.

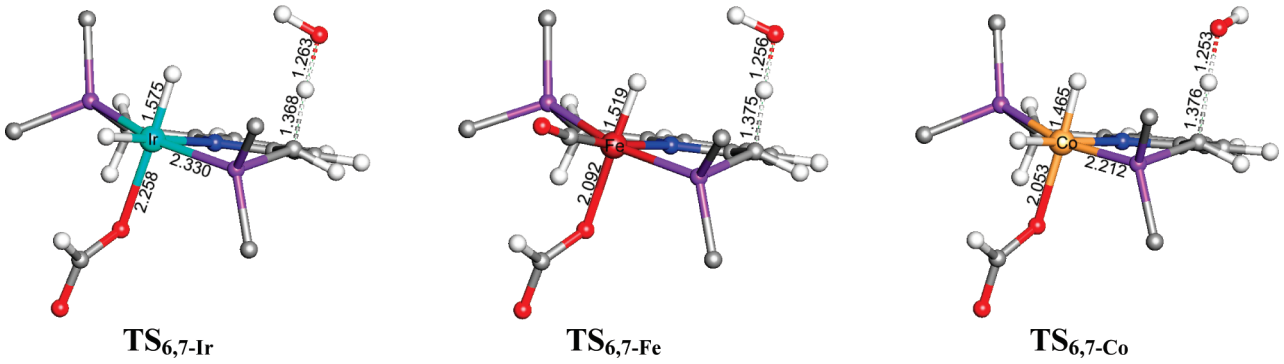

$TS_{6,7\text{-Ir}}$ **$TS_{6,7\text{-Fe}}$** **$TS_{6,7\text{-Co}}$**

Figure 6. Optimized structures of $\mathbf{TS}_{6,7\text{-Ir}}$ ($1496i\ cm^{-1}$), $\mathbf{TS}_{6,7\text{-Fe}}$ ($1498i\ cm^{-1}$), and $\mathbf{TS}_{6,7\text{-Co}}$ ($1505i\ cm^{-1}$). Bond lengths are in angstroms. Iso-propyl groups are not shown for clarity.

are slightly different, current results indicate that these three complexes have similar catalytic reaction pathways. Therefore, the reaction mechanisms for hydrogenation of CO_2 catalyzed by **1-Ir**, **1-Fe**, and **1-Co** are shown in one scheme (Scheme 1). The corresponding enthalpy profiles for different reaction pathways are shown in Figure 2 and 5. Some important transition state structures are shown in Figures 3, 4, 6, 7, 8 and 9.

As shown in Scheme 1 and Figures 2 and 5, the catalytic reaction begins with the attack of a CO_2 molecule to one of the *trans* hydrides in **1**. A hydride is transferred directly from the metal center to the carbon atom in CO_2 through a low-barrier transition state $\mathbf{TS}_{1,2}$ (Figure 3, $\Delta H^{\ddagger}$ = 4.0, 1.9, and 2.3 kcal mol^{-1} for Ir, Fe, and Co, respectively) for the formation of intermediate **2**, in which a $HCOO^-$ group is formed and attaches to the metal center with a M···H distance of 2.153, 1.894, and 1.889 Å for Ir, Fe, and Co, respectively. The direct hydride transfer from **1-Ir** for the formation of $HCOO^-$ was also obtained by Ahlquist[11] for a simplified structure model with a similar enthalpy barrier. The dissociation enthalpies of $HCOO^-$ from **2** for the formation of unstable cation intermediate **3** are only 2.0, 2.7, and 2.6 kcal mol^{-1} uphill for Ir, Fe, and Co, respectively. Depending on which ligand (H_2, $HCOO^-$, or OH^-) coordinates to the vacant position in **3**, there are three possible reaction pathways for the regeneration of catalyst **1**. In the first reaction pathway, a H_2 molecule fills the vacant position in **3** and forms a slightly more stable intermediate **4**. Then an OH^- base attacks the dihydrogen in **4** and forms a water molecule by taking a proton from H_2 through transition state $\mathbf{TS}_{4,5}$ (Figure 4), which is only 17.7, 20.0, and 21.1 kcal mol^{-1} higher than **4** for Ir, Fe, and Co, respectively. The H_2 cleavage product **5** is much more stable than **4** and has a water molecule attached to a hydride by a weak $M-H^{\delta-}\cdots H^{\delta+}-O$ dihydrogen bond with H···H distance close to 1.7 Å. The dissociation of H_2O from **5** for the regeneration of **1** is only about 1.0 kcal mol^{-1} uphill. The calculated total enthalpy release in a catalytic cycle ($CO_2 + H_2 + OH^- \rightarrow HCOO^- + H_2O$) is −18.9 kcal mol^{-1}, which is very close to the enthalpy difference (−19.9 kcal mol^{-1}) obtained from standard thermochemical table.[40] The cationic complex **3** is also likely to have a coordinated water instead of H_2. However, no further reaction toward the regeneration of **1** will happen if a water molecule is coordinated to **3**. The coordination of a water molecule in **3** is only about 1 kcal mol^{-1} more stable than **4** in enthalpy, which indicates a rapid H_2/H_2O exchange in **4**.

The second reaction pathway begins with the reassociation of $HCOO^-$ to **3** for the formation of intermediate **6** with a M−O bond length of 2.257, 2.080, and 2.041 Å for Ir, Fe, and Co, respectively. Then the pyridine ring in **6** can easily be dearomatized by transferring a methylene proton from the PNP ligand to an OH^- base through transition state $\mathbf{TS}_{6,7}$ (Figure 6) with an enthalpy barrier of 25.5, 25.1, and 25.6 kcal mol^{-1} for Ir, Fe, and Co, respectively. The dearomatization product **7** is about 20 kcal mol^{-1} less stable than **6** and has a water molecule attached to an unsaturated carbon through weak C···H interaction. Then the $HCOO^-$ group in **7** can easily be replaced by a H_2 molecule for the formation of **8**. The relative enthalpies between **7** and **8** are only −0.9, 2.1, and 3.0 kcal mol^{-1} for Ir, Fe, and Co respectively, indicating rapid $HCOO^-/H_2$ exchanges under mild conditions. **8** can also be formed from **4** through a proton transfer transition state $\mathbf{TS}_{4,8}$ (Figure 7) with energy barriers very close to $\mathbf{TS}_{6,7}$. The dissociation of H_2O from **8** for the formation of **9** is only 1.8, 1.7, and 2.2 kcal mol^{-1} uphill for Ir, Fe, and Co,

dx.doi.org/10.1021/cs2000329 |ACS Catal. 2011, 1, 849–854

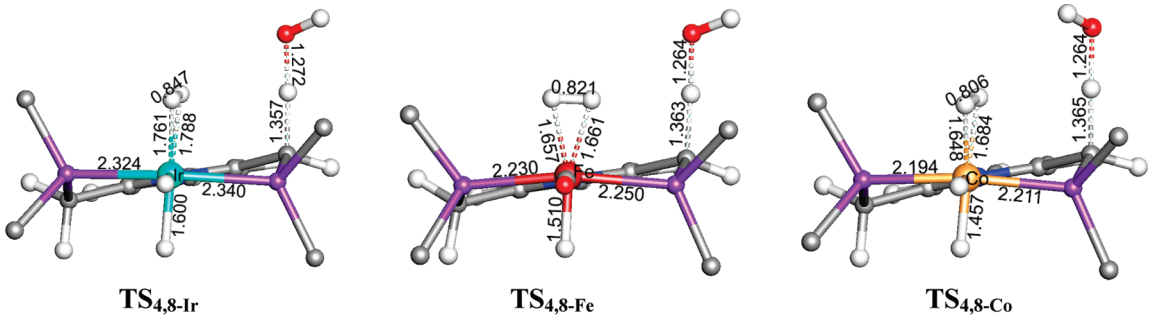

Figure 7. Optimized structures of $\mathbf{TS_{4,8\text{-}Ir}}$ (1474*i* cm^{-1}), $\mathbf{TS_{4,8\text{-}Fe}}$ (1493*i* cm^{-1}), $\mathbf{TS_{4,8\text{-}Co}}$ (1487*i* cm^{-1}). Bond lengths are in angstroms. Iso-propyl groups are not shown for clarity.

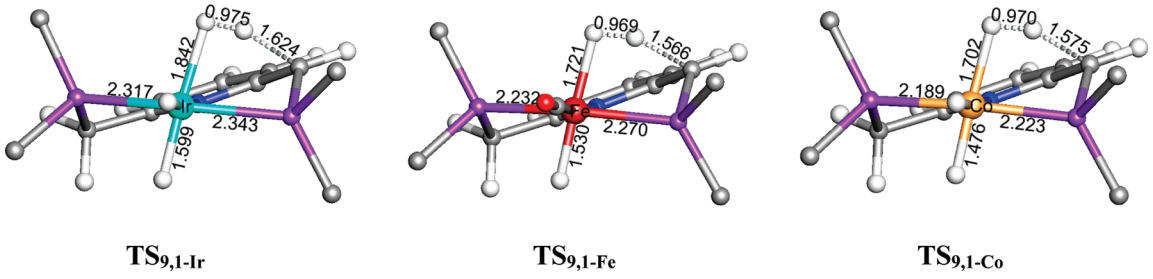

Figure 8. Optimized structures of $\mathbf{TS_{9,1\text{-}Ir}}$ (1394*i* cm^{-1}), $\mathbf{TS_{9,1\text{-}Fe}}$ (1433*i* cm^{-1}), and $\mathbf{TS_{9,1\text{-}Co}}$ (1460*i* cm^{-1}). Bond lengths are in angstroms. Iso-propyl groups are not shown for clarity.

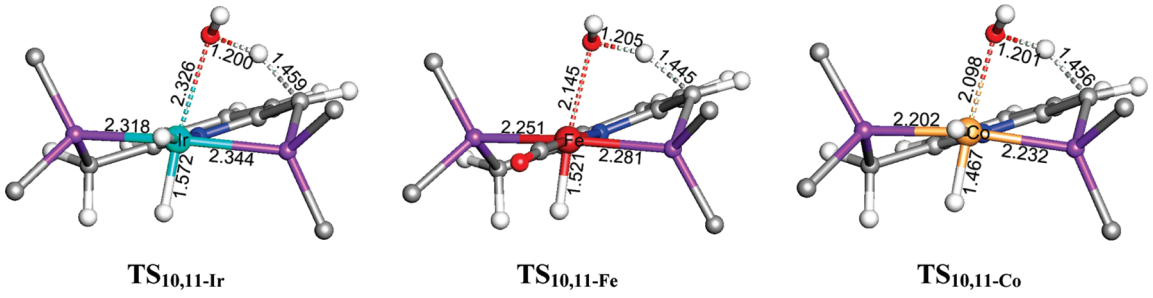

Figure 9. Optimized structures of $\mathbf{TS_{10,11\text{-}Ir}}$ (1486*i* cm^{-1}), $\mathbf{TS_{10,11\text{-}Fe}}$ (1485*i* cm^{-1}), and $\mathbf{TS_{10,11\text{-}Co}}$ (1497*i* cm^{-1}). Bond lengths are in angstroms. Iso-propyl groups are not shown for clarity.

respectively. Finally, the dihydrogen in **9** is split by transferring a proton to the unsaturated carbon in the PNP ligand for the regeneration of **1** through transition state $\mathbf{TS_{9,1}}$ (Figure 8, $\Delta H^{\ddagger}$ = 23.2, 16.6, and 18.6 kcal mol^{-1} for Ir, Fe, and Co) with a total enthalpy barrier ($\mathbf{6} \rightarrow \mathbf{TS_{9,1}}$) of 38.5, 40.0, and 42.5 kcal mol^{-1} for Ir, Fe, and Co, respectively. Such high barriers cannot be achieved under mild conditions.

The third reaction pathway begins with the attack of an OH^- base to the vacant position in **3** for the formation of intermediate **10**, which is very close to **3** in enthalpy. Then a methylene proton in the PNP ligand is transferred to the OH group in **10** for the formation of a H_2O molecule through transition state $\mathbf{TS_{10,11}}$ (Figure 9, $\Delta H^{\ddagger}$ = 15.8, 6.9, and 7.9 kcal mol^{-1} for Ir, Fe, and Co, respectively) with an enthalpy barrier of 19.9, 18.7, and 19.9 kcal mol^{-1} relative to **10** for Ir, Fe, and Co, respectively. Once the H_2O is formed in **11**, H_2O/H_2 exchange happens rapidly for the formation of **9**, which is 4.3, 1.3, and 0.1 kcal mol^{-1} more stable than **11** for Ir, Fe, and Co, respectively. Then **1** can be regenerated through $\mathbf{TS_{9,1}}$.

Comparing all relative enthalpies in the three reaction pathways and considering the formation of stable intermediate **6**, the first reaction pathway with direct H_2 cleavage by OH^- has the lowest overall enthalpy barrier in the catalytic CO_2 hydrogenation cycle. For the experimentally reported Ir catalyst, the overall enthalpy barrier ($\mathbf{6} \rightarrow \mathbf{TS_{4,5}}$) is 18.6 kcal mol^{-1}. Such a low barrier explains the observed unprecedented high activity of **1-Ir** in catalytic hydrogenation of CO_2. For the newly proposed iron and cobalt PNP-pincer complexes, the overall enthalpy barriers ($\mathbf{6} \rightarrow \mathbf{TS_{4,5}}$) are 21.9 and 22.6 kcal mol^{-1}, which are still achievable under mild conditions.

SUMMARY AND CONCLUSIONS

In summary, two hypothetical PNP-ligated base metal pincer complexes, **1-Fe** and **1-Co**, were examined computationally based on the understanding of a recently reported fast CO_2 hydrogenation catalyst, (^{i}PrPNP)IrH_3. When this paper was

dx.doi.org/10.1021/cs2000329 |*ACS Catal.* 2011, 1, 849–854

being finalized, **1-Fe** was synthesized by Milstein and co-workers in their study of hydrogenation of ketones catalyzed by iron pincer complexes.[29] However, **1-Fe** was only made to evaluate its intermediacy in the catalytic hydrogenation of ketones and the catalytic properties of **1-Fe** for hydrogenation of CO_2 were not evaluated. Detailed mechanisms for hydrogenation of CO_2 catalyzed by **1-Ir**, **1-Fe**, and **1-Co** were studied computationally using DFT. Calculation results indicate that the reaction pathway with direct H_2 cleavage by OH^- for the regeneration of the catalyst without the participation of the PNP ligand is about 20 kcal mol^{-1} more favorable than the previously postulated catalytic CO_2 reduction mechanism with dearomatization and rearomatization of the pyridine ring in the PNP ligand for H_2 cleavage, as proposed by Nozaki and co-workers.[10] The OH^- triggered H_2 cleavage transition states are also different as compared with Ahlquist's theoretical study of the Ir catalyst using a simplified structure model.[11] The calculated overall enthalpy barriers (**6** → $\mathbf{TS_{4,5}}$) of **1-Ir**, **1-Fe**, and **1-Co** catalyzed hydrogenation of CO_2 are 18.6, 21.9, and 22.6 kcal mol^{-1}, respectively. Therefore, the newly designed complexes **1-Fe** and **1-Co** are proposed as promising low-cost and high efficiency base metal catalyst candidates for CO_2 reduction. In addition, the predicted reaction mechanism reveals the essential role of the OH^- base in the catalytic cycle and points the way to finding new catalysts, as the strong base and unsaturated ligand may be critical for hydrogen activation and low energy proton transfers.

■ ASSOCIATED CONTENT

Supporting Information. Complete ref 30, evaluation of the solvent effect corrections, and atomic coordinates of all optimized structures. This material is available free of charge via the Internet at http://pubs.acs.org.

■ AUTHOR INFORMATION

Corresponding Author

*E-mail: yangxz@berkeley.edu.

Funding Sources

This work was supported by National Science Foundation (CHE-0840505) and the Molecular Graphics and Computation Facility (Dr. Kathleen A. Durkin, Director) in the College of Chemistry at the University of California, Berkeley.

■ ACKNOWLEDGMENT

I thank Dr. Jason M. Keith (Los Alamos National Lab, Los Alamos, NM) for constructive discussion and help with manuscript preparation.

■ REFERENCES

(1) Aresta, M., Ed.; *Carbon Dioxide as a Chemical Feedstock*; Wiley-VCH: Weinheim, Germany, 2010.
(2) Bakac, A., Ed.; *Physical Inorganic Chemistry*; John Wiley & Sons: NJ, 2010; pp 247−279.
(3) Jessop, P. G.; Ikariya, T.; Noyori, R. *Chem. Rev.* **1995**, *95*, 259.
(4) Jessop, P. G.; Joó, F.; Tai, C.-C. *Coord. Chem. Rev.* **2004**, *248*, 2425.
(5) Dubois, M. R.; Dubois, D. L. *Acc. Chem. Res.* **2009**, *42*, 1974.
(6) Junge, H.; Boddien, A.; Capitta, F.; Loges, B.; Noyes, J. R.; Gladiali, S.; Beller, M. *Tetrahedron Lett.* **2009**, *50*, 1603.
(7) Federsel, C.; Jackstell, R.; Beller, M. *Angew. Chem., Int. Ed.* **2010**, *49*, 6254.
(8) Boddien, A.; Loges, B.; Gärtner, F.; Torborg, C.; Fumino, K.; Junge, H.; Ludwig, R.; Beller, M. *J. Am. Chem. Soc.* **2010**, *132*, 8924.
(9) Loges, B.; Boddien, A.; Gärtner, F.; Junge, H.; Beller, M. *Top. Catal.* **2010**, *53*, 902.
(10) Tanaka, R.; Yamashita, M.; Nozaki, K. *J. Am. Chem. Soc.* **2009**, *131*, 14168.
(11) Ahlquist, M. S. G. *J. Mol. Catal. A: Chem.* **2010**, *324*, 3.
(12) de Vries, J. G.; Elsevier, C. J., Eds.; *Hand Book of Homogeneous Hydrogenation*; Wiley-VCH: Weinheim, Germany, 2007; Vol. 1, p 489.
(13) Tai, C.-C.; Chang, T.; Roller, B.; Jessop, P. G. *Inorg. Chem.* **2003**, *42*, 7340.
(14) Casey, C. P.; Guan, H. *J. Am. Chem. Soc.* **2009**, *131*, 2499.
(15) Mikhailine, A.; Lough, A. J.; Morris, R. H. *J. Am. Chem. Soc.* **2009**, *131*, 1394.
(16) Sui-Seng, C.; Freutel, F.; Lough, A. J.; Morris, R. H. *Angew. Chem., Int. Ed.* **2008**, *47*, 940.
(17) Federsel, C.; Boddien, A.; Jackstell, R.; Jennerjahn, R.; Dyson, P. J.; Scopelliti, R.; Laurenczy, G.; Beller, M. *Angew. Chem., Int. Ed.* **2010**, *49*, 9777.
(18) Siegel, J. B.; Zanghellini, A.; Lovick, H. M.; Kiss, G.; Lambert, A. R.; Clair, J. L., St.; Gallaher, J. L.; Hilvert, D.; Gelb, M. H.; Stoddard, B. L.; Houk, K. N.; Michael, F. E.; Baker, D. *Science* **2010**, *329*, 309.
(19) Nørskov, J. K.; Bligaard, T.; Rossmeisl, J.; Christensen, C. H. *Nat. Chem.* **2009**, *1*, 37.
(20) Houk, K. N.; Cheong, P. H.-Y. *Nature* **2008**, *455*, 309.
(21) Hölscher, M.; Leitner, W. *Chem.—Eur. J.* **2010**, *16*, 14266.
(22) Lu, G.; Li, H.; Zhao, L.; Fang Huang, F.; Schleyer, P.; von, R.; Wang, Z.-X. *Chem.—Eur. J.* **2011**, *17*, 2038.
(23) Hebden, T. J.; John, A. J., St.; Gusev, D. G.; Kaminsky, W.; Goldberg, K. I.; Heinekey, D. M. *Angew. Chem., Int. Ed.* **2011**, *50*, 1873.
(24) Ingleson, M.; Fan, H.; Pink, M.; Tomaszewski, J.; Caulton, K. G. *J. Am. Chem. Soc.* **2006**, *128*, 1804.
(25) Benito-Garagorri, D.; Puchberger, M.; Mereiter, K.; Kirchner, K. *Angew. Chem., Int. Ed.* **2008**, *47*, 9142.
(26) Pelczar, E. M.; Emge, T. J.; Krogh-Jespersen, K.; Goldman, A. S. *Organometallics* **2008**, *27*, 5759.
(27) Trovitch, R. J.; Lobkovsky, E.; Chirik, P. J. *Inorg. Chem.* **2006**, *45*, 7252.
(28) Zhang, J.; Gandelman, M.; Herrman, D.; Leitus, G.; Shimon, L. J. W.; Ben-David, Y.; Milstein, D. *Inorg. Chim. Acta* **2006**, *359*, 1955.
(29) Langer, R.; Leitus, G.; Ben-David, Y.; Milstein, D. *Angew. Chem., Int. Ed.* **2011**, *50*, 2120.
(30) Frisch, M. J. et al. *Gaussian 09*, revision A.02; Gaussian, Inc.: Wallingford, CT, 2010.
(31) Chai, J. -D.; Head-Gordon, M. *J. Chem. Phys.* **2008**, *128*, 084106.
(32) Hehre, W. J.; Ditchfield, R.; Pople, J. A. *J. Chem. Phys.* **1972**, *56*, 2257.
(33) Hariharan, P. C.; Pople, J. A. *Theor. Chim. Acta* **1973**, *28*, 213.
(34) Krishnan, R.; Binkley, J. S.; Seeger, R.; Pople, J. A. *J. Chem. Phys.* **1980**, *72*, 650.
(35) Andrae, D.; Haeussermann, U.; Dolg, M.; Stoll, H.; Preuss, H. *Theor. Chim. Acta* **1990**, *77*, 123.
(36) Martin, J. M.; Sundermann, A. *J. Chem. Phys.* **2001**, *114*, 3408.
(37) Tomasi, J.; Mennucci, B.; Cammi, R. *Chem. Rev.* **2005**, *105*, 2999.
(38) Bondi, A. *J. Chem. Phys.* **1964**, *68*, 441.
(39) Manson, J.; Webster, C. E.; Hall, M. B. *JIMP2*, version 0.091, a free program for visualizing and manipulating molecules; Texas A&M University: College Station, TX, 2006.
(40) Wagman, D. D.; Evans, W. H.; Parker, V. B.; Schumm, R. H.; Halow, I. *The NBS Tables of Chemical Thermodynamic Properties: Selected Values for Inorganic and C1 and C2 Organic Substances in SI Units*; American Chemical Society and the American Institute of Physics for the National Bureau of Standards: New York, 1982.